Leadership in Sustainable Infrastructure
Leadership en Infrastructures Durables

Vancouver, Canada
May 31 – June 3, 2017/ *Mai 31 – Juin 3, 2017*

EFFECT OF GFRP BAR SPLICE LENGTH ON FEXURAL STRENGTH OF JOINTED PRECAST DECK SLAB WITH UHPFRC-FILLED CLOSURE STRIP

Sherif, Mohtady[1,3] and Sennah, Khaled[2]
[1,2] Ryerson University, Canada
[3] mohtady.sherif@ryerson.ca

Abstract: Glass fiber reinforced polymer (GFRP) bars are used in bridge decks to overcome the problem of corrosion of steel bars and concrete spalling. However, design guidelines for joints between GFRP-reinforced precast deck panels supported over girders for accelerated bridge replacement is as yet unavailable. The proposed research investigates the use of GFRP bars in the closure strip between jointed precast deck panels, which is filled with ultra-high performance fiber-reinforced concrete (UHPFRC). Four different bar lap splice lengths in the joint were considered in this study, namely: 75, 105, 135 and 165 mm. Four specimens were constructed and tested to-collapse to determine their structural behavior and load carrying capacity. Correlation between experimental findings and available design equations for moment and shear capacities was conducted, leading to recommendations for the use of the proposed joints between precast deck panels in slab-on-girder bridges.

1 INTRODUCTION

Bridges are a major component of any infrastructure, acting as critical links in most of the road networks and railways, connecting cities and countries and securing a critical mean of transportation of goods and people from place to another. Such vital asset requires routine inspection, maintenance and as problems arise, the demand for research, innovation and development of new materials, structural components, applications, and construction methods increase. In Canada, severe weather fluctuations in winter times result in freezing and thawing of structural members and the use of deicing salts makes the expansive corrosion of steel reinforcement in bridge deck slabs a major issue. This leads to reduction in the capacity and the life expectancy of bridges, costly routine maintenance and in some cases replacement of the bridge or the severely deteriorated components. From engineering and economic perspectives, for the process of replacing the deteriorated bridge or some of its components to be effective, it should have a minimal impact on the traffic. Also, it should incorporate innovative materials and construction techniques that will limit or minimize the effect of deicing salt used in winter times in Canada.

The federal highway administration (FHWA) defines accelerated bridge construction (ABC) as making use of innovative planning, design, materials, and construction methods in a safe and cost-effective manner to reduce the onsite construction time that occurs when building new bridges or replacing and rehabilitating existing bridges (Culmo 2009). ABC results in improved site constructability, total project delivery time and work zone safety for travelling public. It also reduces the impact on traffic, and the weather-related time delays, maintaining and/or improving construction quality, and reducing the life cycle costs and environmental impacts. Prefabricated components can be delivered to site and quickly assembled, and thus they can reduce design and constriction time and cost, minimize forming, minimize lane closure time and/or possibly eliminate the need for a temporary bridge. Recent surveys of the state of practice of full-depth, full-width panel-girder system and joints were conducted elsewhere (PCI, 2011; NCHRP, 2011; Badie and Tadros, 2008; Hieber and Wacker, 2005). Few authors have dealt with panel-to-panel

longitudinal joints in bulb-tee girder (Sennah and Afifi, 2015, Afefy et al., 2015; Li et al., 2011; Graybeal, 2010). While others authors have dealt with panel-to-panel transverse joints (Culmo, 2011; Graybeal, 2010; Issa el al., 2006). Zhu et al. (2012) proposed continuous transverse U-bar joint details, incorporating projecting reinforced steel bars from the jointed panels which can provide negative moment continuity in multi-span bridges, however no pretensioning was used. One of the ABC techniques is the use of prefabricated systems to minimize the use of the conventional cast-in-place techniques. A major component of such system, which is the focus of this research, is the jointed prefabricated deck panels that are supported over either steel or prefabricated precast concrete girders. Figure 1(a) depicts a schematic diagram of precast full-depth deck panels placed transversally over girders. While Figure 1(b) presented the bulb-tee pretentioned girders placed side-by-side over abutments and piers and jointed together at the level of the deck slab.

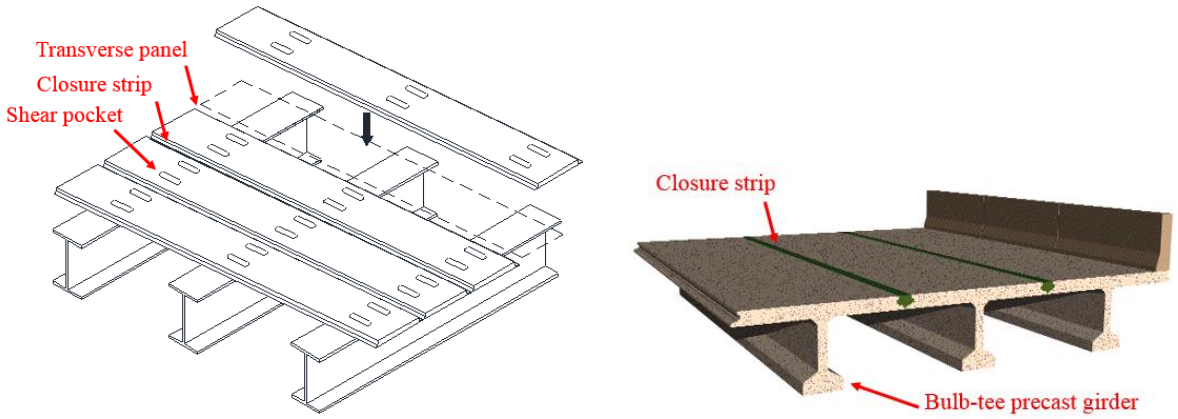

a) Transverse panels placed over girders b) Bulb-tee precast girders with closure strips

Figure 1: Views of two types of prefabricated bridge systems to accelerate bridge construction

2 SIGNIFICANCE OF THIS RESEARCH

Several research studies been conducted on the behavior of the joint between the precast prefabricated deck panels considering conventional steel reinforcement, epoxy-coated steel bars and GFRP bars. Summary of these studies can be found elsewhere (Culma, 2009; Khalafalla and Sennah, 2015; Sayed Ahmed and Sennah, 2016). These studies investigated the reinforcement details in the joint such as bent bars, bars with hooked ends, headed- and straight-end bars, combined with different shear key shapes and different joint filling materials, such as non-shrinking grout, high performance concrete (HPC) and ultra-high performance fiber reinforced concrete (UHPFRC). Among the materials being proposed and investigated in the jointed precast deck panels, the ribbed-surface GFRP bars and UHPFRC are of a growing interest and focus. The outstanding properties of each of these materials eliminate the durability issues that existed when using steel reinforcement and allow for expansion on accelerated bridge construction practice. However, literature survey showed that neither the Canadian Highway Bridge Design Code (CHBDC, 2014), nor the AASHTO-LRFD Specifications for Design of Highway Bridges (AASHTO-LRFD, 2012), provide guidance of the design of the joints of prefabricated deck slabs reinforced with GFRP and UHPFRC. Also, the most recently-developed AASHTO Bridge Design Guide Specifications for GFRP-Reinforced Concrete Bridge Decks and traffic Railings (AASHTO, 2009) does not provide guidance on the design of closure strips between GFRP-Reinforced precast deck panels. So this research addresses expects to provide guidance for the design of such jointed slabs when subjected to dead load and truck loading conditions. The proposed experimental program provides data to assist in obtaining the precast deck slab capacity based on the joint details as affected by joint width and associated bar splice length.

3 RESEARCH OBJECTIVES

The objective of this research was to conduct a parametric study using experimental testing to investigate the behavior of ribbed-surface GFRP bars in the closure strip between jointed precast deck slabs resting

over steel or concrete girders. The experimental findings were then be correlated with the available theoretical moment and shear capacities of the slab cross-section to examine their applicability. Finally, for design purposes, the maximum spacing between girders to be considered to use the developed joints in practice were determined based on CHBDC applied factored dead and live load moments.

4 EXPERIMENTAL PROGRAM

4.1 Test Matrix and Key Parameters

This experimental study was composed of 4 one-way slabs simulating a 600-mm width of the deck slab between bridge girders. The slabs had a fixed spacing of bars in the lap splice and main bar spacing with bar splice length of 75, 105, 135 and 165 mm for closure strip widths of 125, 155, 185 and 215 mm, respectively as per Table 1. It should be noted that target compressive strengths of precast concrete and UHPFRC were 35 and 160 MPa, respectively. More details about the characteristics of the used UHPFRC can be found elsewhere (Sherif, 2017).

Table 1: Test matrix

Slab Dimensions (mm)	Slab No.	Joint Width	Splice Length	f'c (MPa)		Splice Configuration		Bar Spacing
				Precast	Joint	Type	Offset (mm)	
2800×600×200	S1	125	75	35	160	Contact	0	200
	S2	155	105					
	S3	185	135					
	S4	215	165					

4.2 Specimens Description and Test Setup

Each of the tested slab had a 2800 mm total length and 2400 mm effective span length between supports. The slab thickness and width are 200 and 600 mm, respectively, as depicted in Figure 2. Each of the test specimens considered contact lap splice where the spacing between the two bars in the lap splice is zero (i.e. contact or overlapped splice). GFRP bars of 16M size were used to reinforce the slab in its tension side at 200 mm. The widths of the closure strip were taken as 125, 155, 185 and 215 mm for slabs S1, S2, S3, and S4, respectively, on which the projecting bar length of 25 mm short of the joint width to allow for construction tolerance. The shape of the joint is a typical shear key as depicted in Figure 2(b). The tensile strength and modulus of elasticity of the bars were 1188 MPa and 64 GPa, respectively, tensile strain at rupture of 1.86% (Schoeck, 2013). Two bar sizes were considered in this study, namely: 12M and 16M bars with nominal cross-sectional area of 113 and 201 mm^2, respectively. The main tension reinforcement and bottom transverse reinforcement the slabs were considered of 16M bar, while top mesh was considered of 12M bars. More details of the experimental program can be found elsewhere (Sherif, 2017). A four-point loading test setup was used in this study in order to expose the joint to pure flexure. Each slab was simply-supported over steel pedestals. A hinged support was utilized at the left support line using a steel rod sandwiched between two grooved steel plates while at the right support line, a roller support was formed on top of the pedestal using a steel rod sandwiched between two flat steel plates. Two linear variable displacement transducers (LVDTs) were installed at the mid-span to measure the deflection as depicted in Figure 3. The load was applied gradually in increments of 10 kN till failure so that initiation of cracks and crack propagation were recorded. A data acquisition system was used to collect data from sensors during the test. After each test, data collected from sensors were analyzed and presented in graphical format for further discussions.

5 EXPERIMENTAL RESULTS

Concrete cylinder specimens were tested to-collapse at the time of each test to determine the average compressive strength of normal-strength concrete as well as UHPFRC. Table 2 summaries the results from these tests for each slab.

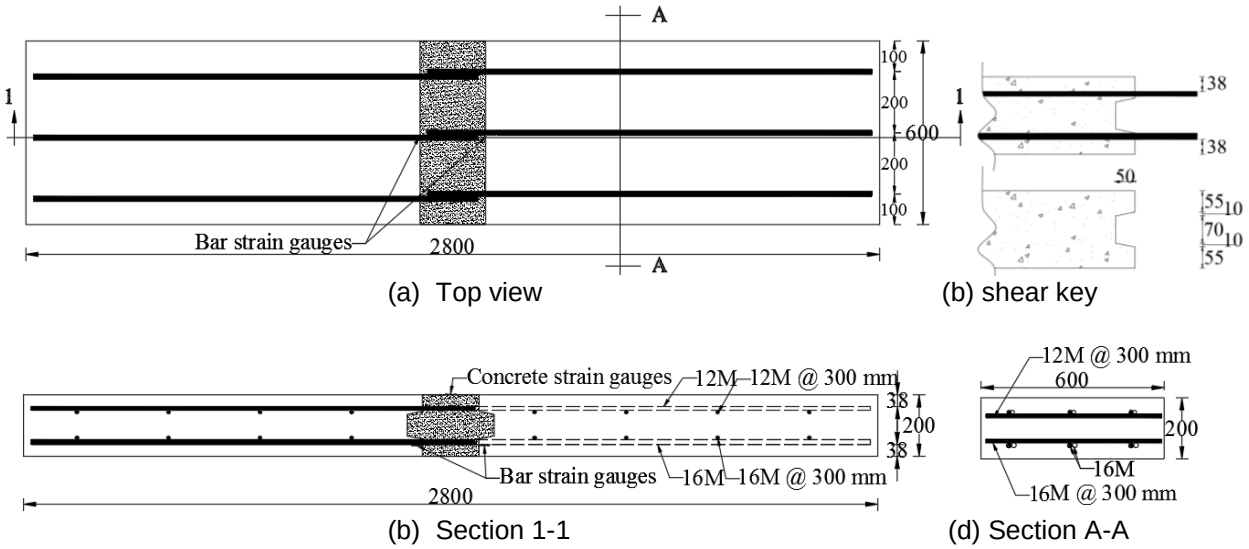

Figure 2: Typical dimensions, joint configuration and GFRP bar arrangement for the slabs

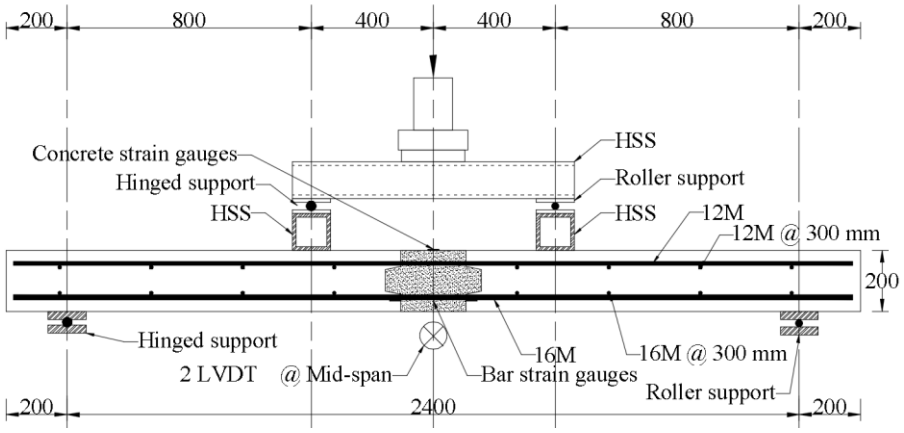

Figure 3: Test setup

Table 2: Summary of concrete compressive strength results

Slab	Precast panels (MPa)	UHPFRC joint (MPa)
S1	44.60	122.30
S2	47.40	179.90
S3	45.63	164.63
S4	44.60	160.90

5.1 Failure Modes and Sensor Data

The jointed slab S1 with splice length of 75 mm and joint width of 125 mm was tested to-collapse. The first flexural crack was observed at the interface between the precast concrete and the UHPFRC-filled joint at 21.35 kN. This crack continued propagating upward along the interface of the joint and the precast slab with increase in applied load. Other flexural cracks within the precast slab started to appear between the quarter points of the slab and continued propagating towards the top of the slab causing flexural failure at an ultimate load of 99.34 kN. View of crack pattern at failure for specimen S1 is shown in Figure 4. The jointed slab S2 with splice length of 105 mm and joint width of 155 mm was tested to-collapse. The first flexural crack was observed at the interface between the precast concrete and the UHPFRC-filled joint at 23.65 kN. This crack continued propagating upward along the interface of the joint and the precast slab

with increase in applied load as depicted. Other flexural cracks within the precast slab started to appear between the quarter points of the slab and continued propagating towards the top of the slab causing flexural failure at an ultimate load of 120.32 kN as shown in Figure 4.

Jointed slab S3 with splice length of 135 mm and joint width of 185 mm was tested to-collapse. The first flexural crack was observed at the interface between the precast concrete and the UHPFRC-filled joint at 22.80 kN. This crack continued propagating upward along the interface of the joint and the precast slab with increase in applied load. Other flexural cracks within the precast slab started to appear between the quarter points of the slab and continued propagating towards the top of the slab with increase of applied load. Also, other diagonal cracks appeared just beside the point load on the support side and propagated further in the slab thickness till reaching a sudden flexural-shear failure at an ultimate load of 135.74 kN. Figure 4 shows view of the crack pattern of slab S3 after failure. Jointed slab S4 with splice length of 165 mm and joint width of 215 mm was tested to-collapse. The first flexural crack was observed at the interface between the precast concrete and the UHPFRC-filled joint at 23.55 kN. This crack continued propagating upward along the interface of the joint and the precast slab with increase in applied load. Other flexural cracks within the precast slab started to appear between the quarter points of the slab and continued propagating towards the top of the slab with increase of applied load. Also, other diagonal cracks appeared just beside the point load on the support side and propagated further in the slab thickness till reaching a sudden flexural-shear failure at an ultimate load of 131.82 kN as depicted in Figure 4.

Figures 4 and 5 show the cracking pattern from the two sides of slabs S1, S2, S3 and S4 when stacked on top of each other. One may observe that with increase in bar splice length and hence the joint width, the failure mode changed from pure flexural to combined flexural and shear. When comparing results for slabs S1 and S2 of the same failure mode, it can be observed that the increase of splice length from 75 to 105 mm increased the slab capacity by 21%. Also, when comparing results for slabs S2 and S3, it can be observed that the increase of splice length from 105 to 135 mm increased the slab capacity by 13% and changed the failure mode from flexural to combined-flexure and shear. Moreover, when comparing results for slabs S3 and S4, it can be observed that the increase of splice length from 135 to 165 mm showed slight change in the load carrying capacity of 3% while the failure mode remained unchanged. The slight difference of 3% may be attributed to the slight difference in compressive strength of the concrete materials as depicted in Table 2. So, it can be concluded that the load carrying capacity of the slab may remain unchanged increase in splice length beyond 135 mm and hence the joint width beyond 185 mm. In slabs S1 and S2, one may observe that the flexural crack at the interface between the UHPFRC and the precast slab was too wide to the extent that bar slip from the UHPFRC occurred. To investigate this hypnosis, a core sample was taken from each slab and then sliced at the bar location to examine whether the bar slipped from concrete. Figures 6 and 7 show views of the sliced core sample showing the end of the GFRP bar slipped from concrete at its end as well as shearing of bar ribs, respectively.

Table 3: Summary of concrete compressive strength results

Slab	Cracking Load	Cracking moment	Ultimate load	Ultimate moment	Ultimate shear	Failure Mode
	kN	kN.m	kN	kN.m	kN	
S1	21.35	8.54	99.34	39.74	49.67	Flexure
S2	23.65	9.46	120.32	48.13	60.16	Flexure
S3	22.80	9.12	135.74	54.30	67.87	Flexural-shear
S4	23.55	9.42	131.82	52.73	65.91	Flexural-shear

Figure 8 depicts the applied moment-deflection relationship for the tested slabs. It can be observed that the maximum mid-span deflection increases with increase in joint width when failure mode is flexural, as expected. Figure 9 shows the relationship between the applied moment and the maximum concrete strain at top of the slab. One may observe that the maximum concrete strains for slabs S1 and S2, which failed in flexure, are 258 and 457 micro-strain. These values are far below the concrete failure micro-strain of 3500, confirming the flexural failure resulted from bar slip from UHPFRC in the closure strip and rib shearing as depicted in Figure 7. Figure 11 depicts the relationship between the applied moment and bar strain at

the joint-precast slab interface. One may observe that the maximum strain values were 1.6%, 1.8%, 2.3% and 2.2% for slabs S1, S2, S3 and S4, respectively. The corresponding failure stress on the bars were 1034, 1141, 1475 and 1406 MPa for slabs S1, S2, S3 and S4, respectively.

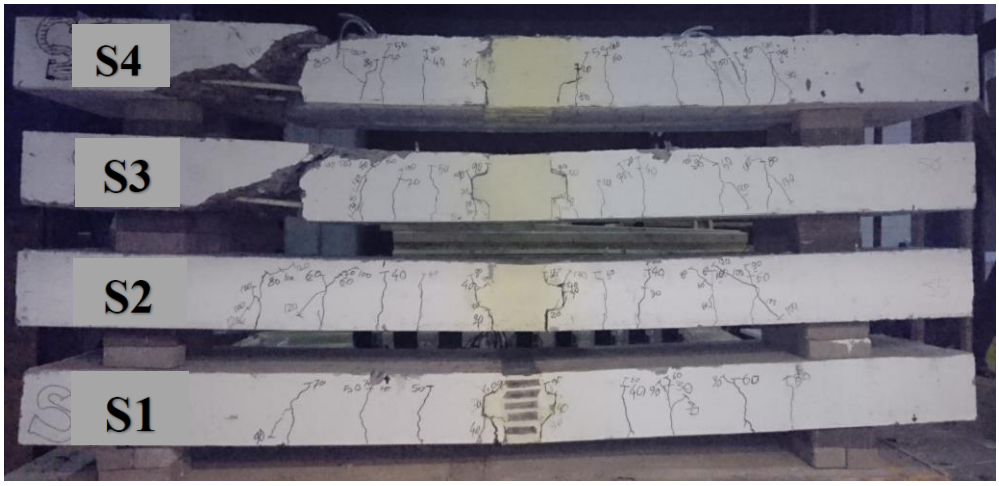

Figure 4: View of failure modes of the slabs from side 1

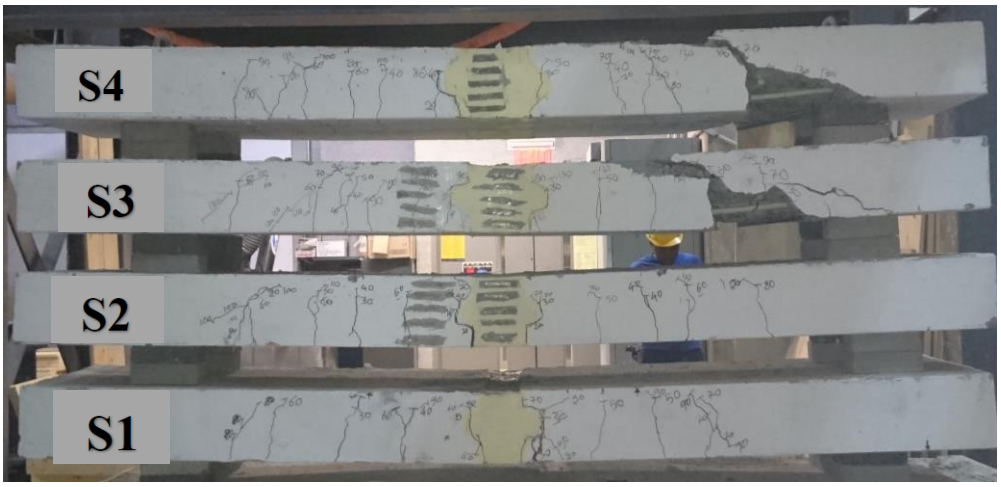

Figure 5: View of failure modes of the slabs from side 2

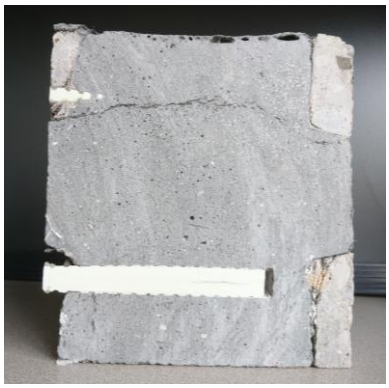
Figure 6: View of bar slippage in a sliced core sample

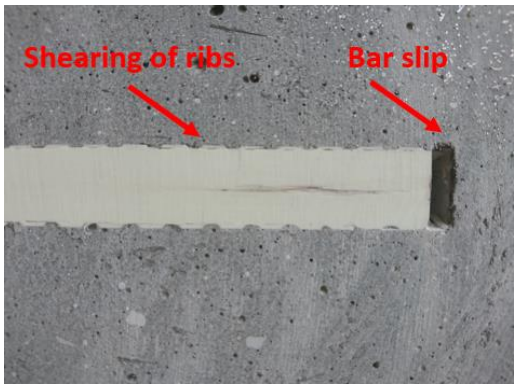

Figure 7: View of bar slippage failure due to shearing of the bar ribs and bar slip

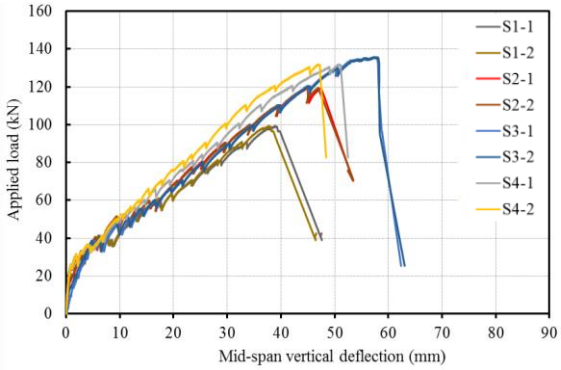

Figure 8: Moment vs deflection relationship for tested slabs

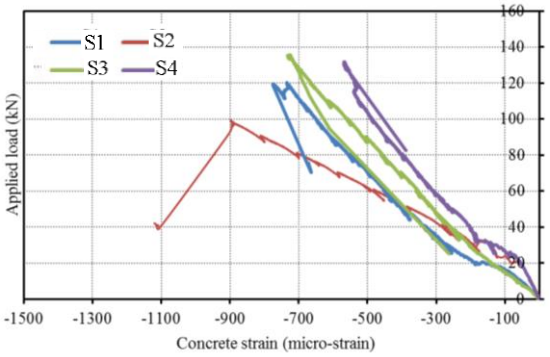

Figure 9: Load-concrete strain relationship for the tested slabs

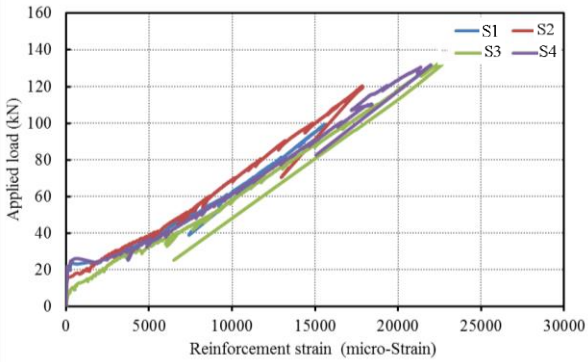

Figure 10: Load-bar strain relationship for the tested slabs

5.2 Theoretical Moment and Shear Capacities

Theoretical moment and shear capacities for the precast slabs were calculated based on ISIS Canada manual No. 3 (ISIS, 2007) and CHBDC of 2014. The capacities were calculated using spreadsheets programed based on the equations and procedures presented in the above-mentioned references. These capacities were obtained considering resistance factors for concrete and GFRP bars of 0.75 and 0.55, respectively. However, the experimental capacity requires a matching resistance factor for the sake of comparison. Chapter 2 of CHBDC (2014) specifies that the designer shall consider the environmental conditions and deterioration mechanisms for the FRP reinforcement. Clause 16.4 in Chapter 16 of CHBDC refer to durability of GFRP without considering a value for the durability factor to be taken in design. On the other hand, Clause 16.5.3 specifies resistance factors to be considered in design calculations. Such resistance factors are generally associated with uncertainty in material's mechanical properties obtained from standard mechanical test method (i.e. tensile strength test method for example). Since the publication of the previous edition of the CHBDC, it is now recognized that the variability of the strength of FRPs is affected more by environmental exposure than by geometric properties and stress levels. It is for this reason that experts in the structural use of FRP are now suggesting that the resistance factors for FRPs should be specified as products of a "material" factor and an "environmental" factor (ACI 440, 2002; Karbhari, 2000). However, Clause 16.4 in CHBDC commentaries states that findings from analyses of available data in the literature have confirmed that the concerns about the durability of GFRP in alkaline concrete, based on simulated laboratory studies in alkaline solutions, are unfounded. Thus, the resistance factor for design calculations of GFRP in CHBDC was 0.75, as given in CHBDC Commentaries, which was mainly drawn from the Japanese document (JSCE, 1997). Table 4 present the factors of safety for the design of the proposed joint details in the tested slabs as the ratio between the experimental moment resistance and the theoretical resistance moment as well as the ratio between the experimental shear resistance and the theoretical shear resistance GFRP when a durability factor of 0.75 is introduced to the experimental findings and the code resistance factors are applied to code theoretical equations for resisting moment and shear forces. One may observe that the factors of safety in pure shear capacity in the right column in the table is always more than 1. However, the factors of safety for moment is less than 1 for the jointed slabs. This may

be attributed to the fact that the moment capacity was calculated for the GFRP-reinforced concrete section just outside the joint considering full bond between the GFRP bars and concrete. This criteria of full bond between the bar and concrete may not be applicable herein since the jointed slabs with pure flexural failure exhibited very wide flexural crack at the joint-precast slab interface, indicating bar slip from UHPFRC at slab failure. Also, the factor of safety for only pure moment capacity may not apply to slabs failed in combined flexure and shear. Thus, for design purposes, the experimental findings can directly be compared to the applied factored moment in the deck slab due to dead and live loads to obtain the maximum span between girders so that Design Engineers can implement one of the developed joint details in their projects. The follows section presents the procedure to achieve this task.

Table 4: Summary of experimental moment and shear compared to theoretical values

Slab	Experimental results/m			Theoretical Moment			Theoretical Shear		
	Failure mode	M_{Exp}/m	V_{Exp}/m	M_r	$\frac{M_{Exp}}{M_r}$	$\frac{0.75\,M_{Exp}}{M_r}$	V_r	$\frac{V_{Exp}}{V_r}$	$\frac{0.75V_{Exp}}{V_r}$
		kN.m/m	kN	kN			kN		
S1	Flexure	66.23	82.78	84.98	0.78	0.58	71.03	1.17	0.87
S2	Flexure	80.21	100.27	87.41	0.92	0.69	73.23	1.37	1.03
S3	Flexural-shear	90.49	113.12	85.89	1.05	0.79	71.85	1.57	1.18
S4	Flexural-shear	87.88	109.85	84.98	1.03	0.78	71.03	1.55	1.16

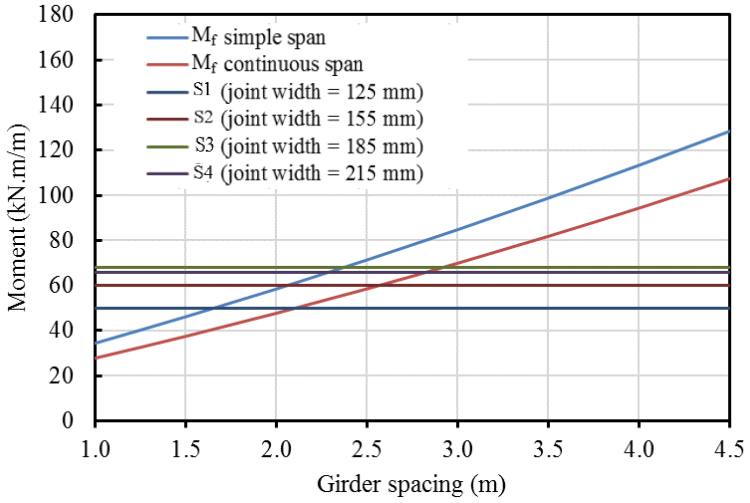

Figure 11: Specified maximum spacing between girders for jointed slabs

5.3 Design Charts for Moment Capacity

It can be observed that the slab capacity increases with increase in joint width. As such, it was decided to be calculated the maximum served span between longitudinal girders in slab-on-girder bridges by comparing the applied factored moment in deck slab due to dead and live load with the experimental values. The applied transverse live load moment for simple slab and continuous slabs were calculated according to Section 5 of CHBDC. Thus, the factored applied moment, M_f, is taken as summation of the factored dead load moment and live load moment. The factored dead load moment includes the moment from the weight of the deck slab and the asphalt layer. The slab thickness considered in this study was 200 mm with unit weight of concrete of 24 kN/m^3 and dead load factor of 1.2. The asphalt layer was assumed of 90 mm thickness and unit weight of 23.5 kN/m^3 with dead load factor of 1.5. The wheel load for live load moment calculations was 87.5 kN with dynamic load allowance of 0.4 and live load factor of 1.7. The applied factored moment in deck slab was calculated for slab spans ranging from 1 to 4.5 m with 0.5 increments. Two deck slab conditions were considered in this study, namely: simple span deck span supported over two girders

and deck slab continuous over 3 of more supports. A reduction factor of 0.8 was applied to the live load moment for continuous span deck slab per CHBDC. On the other hand a durability/resistance factor of 0.75 was applied to the experimental resisting moment that was normalized to be per meter width rather than the actual slab width considered in the tested slab. Figure 11 shows comparison between the applied factored moments for simple span and continuous span deck slabs against the modified experimental findings for girder spacing ranging from 1 to 4.5 m. From these figures, limiting girder spacing was determined for each joint configuration as the point of intersection of the factored applied moment and the resisting moment obtained experimentally. This data was then summarized in Table 5 to assist engineers in selecting the proper joint type per the girder spacing in their bridge project. The use of this data is limited to the materials and geometric conditions in this research. Also, some potential factors of interest could not be addressed in this study. So, bridge designers are expected to include these factors in their design.

Table 5: Specified maximum spacing between girders for jointed slabs

Slab	Splice spacing	Main bar spacing	Splice length	Joint width	Girder spacing limit	
					Inner portion of simple span	Inner portion of continuous span
	mm	mm		mm	M	m
S1	0	200	105	125	1.65	2.10
S2			135	155	2.09	2.58
S3			165	185	2.35	2.91
S4			75	215	2.30	2.85

6 CONCLUSIONS

Glass fiber reinforced polymer (GFRP) bars are used in bridge decks to overcome the problem of corrosion of steel bars and concrete spalling. However, design guidelines for joints between GFRP reinforced precast deck panels supported over girders for accelerated bridge replacement is as yet unavailable. The proposed research investigates the use of GFRP bars in the closure strip between jointed precast deck panels, which is filled with ultra-high performance fiber reinforced concrete (UHPFRC). Four different bar splice lengths in the joint were considered in this study, namely: 75, 105, 135 and 165 mm. Four specimens were constructed and tested to-collapse to determine their structural behavior and load carrying capacity. Correlation between experimental findings and available design equations for moment and shear capacities was conducted, leading to recommendations for the use of the proposed joints between precast deck panels in slab-on-girder bridges.

Based on experimental findings and theoretical analysis, the following conclusions can be drawn:

1- The capacity of the jointed slabs increase as a result of increasing the bar splice length in the joint. Similar conclusion can apply to the bar development length into the joint as well as the joint width.
2- With increase in bar splice length, slab failure mode changed from flexural failure due to bar slip and rib shearing in UHPFRC-filled joint to flexural-shear failure between the joint and the support.
3- Design table specifying the girder spacing limits for each joint configuration was developed based on the moment capacity of each tested jointed slab and the applied factored moment in bridge deck due to dead and live loads. This would assist engineers in selecting the proper joint type per the girder spacing in their bridge project. The use of this data is limited to the materials and geometric conditions in this research. Also, some potential factors of interest could not be addressed in this study. So, bridge designers are expected to include these factors in their design.

7 ACKNOWLEDGEMENTS

The authors would also like to acknowledge the support of Fiberline Composites Canada Inc. and Lafarge Lafarge North America Inc. to this project.

8 REFRENCES

AASHTO. 2009. AASHTO-LRFD Bridge Design Guide Specifications for GFRP-Reinforced Concrete Bridge Decks and Traffic Railings. American Association of State Highway and Transportation Officials. Washington D.C

AASHTO. 2014. AASHTO LRFD Bridge Design Specifications. American Association of State Highway and Transportation Officials. Washington D.C

ACI 440.2R-08. 2008. Guide for the Design and Construction of Externally Bonded FRP Systems for Strengthening Concrete Structures: 45. American Concrete Institute. Farmington Hills, Michigan.

Afefy, H., Sennah, K., Tu, S., Ismail, M., and Kianoush, R. 2015. Experimental Study on the Ultimate Capacity of Deck Joints in Prefabricated Concrete Bulb-Tee Bridge Girders. Journal of Bridge Structures, Design, Assessment and Construction, 11 (2015) 55–71.

Badie, S., and Tadros, M. 2008. Full-Depth Precast Concrete Bridge Deck Panel Systems. NCHRP Report 584, Transportation Research Board, Washington, D.C.

CHBDC. 2014. Canadian Highway Bridge Design Code, CAN/CSA-S6-14. Canadian Standard Association, Toronto, Ontario, Canada.

Culmo, M. P. 2009. Connection Details for Prefabricated Bridge Elements and Systems. Report No. FHWA-IF-09-010., Federal Highway Administration, 568 pages.

Culmo, M. P. 2011. Accelerated Bridge Construction - Experience in Design, Fabrication and Erection of Prefabricated Bridge Elements and Systems. Report FHWA-HIF-12-013, Federal Highway Administration, McLean, VA, USA.

Graybeal, B. 2010. Behavior of Field-Cast Ultra-High Performance Concrete Bridge Deck Connections under Cyclic and Static Structural Loading. Federal Highway Administration, Report No. FHWA-HRT-11-023, 106 pp.

Hieber, D., and Wacker, J. 2005. State-of-the-Art Report on Precast Concrete Systems for Rapid Construction of Bridges. Report No. WA-RD 594.1, Washington State Department of Transportation, 112 pages.

ISIS. 2007. Reinforcing Concrete Structures with Fibre Reinforced Polymers, Design Manual No.3, Intelligent Sensing for Innovative Structures, ISIS Canada. University of Manitoba, Manitoba, Canada.

Issa, M., Salas, J., Shabila, H., and Alrousan, R. 2006. Composite Behavior of Precast Concrete Full-Depth Panels and Prestressed Girders. PCI Journal, 132-145.

JSCE. 2001. Recommendations for Upgrading of Concrete Structures with Use of Continuous Fiber Sheets. JSCE Concrete Engineering Series, Tokyo, 41: 31-34.

Karbhari, V.M. 2000. Determination of Materials Design Values for the Use of Fibre-Reinforced Polymer Composites in Civil Infrastructure. Proceedings of the Institution of Mechanical Engineers - Materials and Design. 214 (Part L): 163–171.

Khalafalla, I., and Sennah, K. 2015. Fatigue Behavior of a Developed UHPC-Filled Precast Deck Joint in Bulb-Tee Bridge Girder System Reinforced with Sand-coated GFRP Bars. Proceedings of the CSCE Annual Conference, Canadian Society for Civil Engineering, Regina, SK, pp. 1-10.

Li, L., Ma, Z., Griffey, M., Oesterle, R. 2011. Improved Longitudinal Joint Details in Decked Bulb Tees for Accelerated Bridge Construction: Concept Development, J. of Bridge Engineering, 15(3): 327-336.

NCHRP. 2011. Summary of Cast-In-Place Concrete Connections for Precast Deck Systems. Research Results Digest 355, Transportation Research Board, pp. 1-33.

PCI. 2011. PCI State-of-the-Art Report on Full-Depth Precast Concrete Bridge Deck Panels (SOA-01-1911), PCI Committee on Bridges and the PCI Bridge Producers Committee, Precast/Prestressed Concrete Institute. Chicago, IL.

Sayed Ahmed, M., and Sennah, K. 2016. Fatigue Strength of Angle-shaped Transverse Connection for GFRP-reinfroced Precast Full-depth Deck Panels in Accelerated Bridge Construction. Proceedings of the 5th International Structural Specialty Conference, CSCE, London, Ontario, pp. 1-9.

Schoeck Canada.2013. “Schöck ComBAR technical information.” http://www.schoeck.ca (Jul. 14, 2013).

Sennah, K., and Afefy, H. 2015. Development and Study of Deck Joints in Prefabricated Concrete Bulb-Tee Bridge Girders: Conceptual Design. Journal of Bridge Structures, Design, Assessment and Construction, 11 (2015) 33–53.

Sherif, M. 2017. Flexural Strength Prediction of Closure Strip between Prefabricated Deck Slabs Supported Over Bridge Girders Incorporating GFRP Bars and UHPFRC. M.A.SC. Thesis, Ryerson University, Toronto, Ontario, Canada.

Zhu, P., Ma, Z., Cao, Q., and French, C. 2012. Fatigue Evaluation of Transverse U-Bar Joint Details for Accelerated Bridge Construction. Journal of Bridge Engineering, 17:191-200.